Carbohydrate Polymers 101 (2014) 878–885

Contents lists available at ScienceDirect

Carbohydrate Polymers

journal homepage: www.elsevier.com/locate/carbpol

Kenaf bast cellulosic fibers hierarchy: A comprehensive approach from micro to nano

Samaneh Karimi[a,*], Paridah Md. Tahir[a], Ali Karimi[a,b], Alain Dufresne[c], Ali Abdulkhani[b]

[a] Laboratory of Biocomposite Technology, Institute of Tropical Forestry and Forest Products (INTROP), University Putra Malaysia, 43400 Serdang, Selangor, Malaysia
[b] Department of Wood and Paper Science and Technology, Faculty of Natural Resources, University of Tehran, P.O. Box 31585-43114, Karaj, Iran
[c] Grenoble Institute of Technology, The International School of Paper, Print Media and Biomaterials (PAGORA), BP65, 38402 Saint Martin d'Hères Cedex, France

ARTICLE INFO

Article history:
Received 28 August 2013
Received in revised form
24 September 2013
Accepted 27 September 2013
Available online 16 October 2013

Keywords:
Kenaf bast
Unbleached nanofiber
Bleached nanofiber
Mechanical defibrillation
Characterization

ABSTRACT

Cellulosic fibers from kenaf bast were isolated in three distinct stages. Initially raw kenaf bast fibers were subjected to an alkali pulping process. Then pulped fibers undergone a bleaching process and finally both pulped and bleached fibers were separated into their constituent nanoscale cellulosic fibers by mechanical shearing. The influence of each treatment on the chemical composition of fibers was investigated. Moreover morphology, functional groups, crystallinity, and thermal behavior of fiber hierarchy at different stages of purification were studied using scanning and transmission electron microscopies, Fourier transform infrared spectroscopy (FTIR), X-ray diffraction (XRD) and thermogravimetric analysis (TGA), respectively. Microscopy studies revealed that applied procedures successfully isolated nanoscale cellulosic fibers from both unbleached and bleached pulps. Chemical composition analysis and FTIR spectroscopy showed that lignin and hemicellulose were almost entirely removed by the applied treatments. XRD and TGA analyses demonstrated progressive enhancement of properties in fibers, hierarchically, in going from micro to nano scale. Interestingly no significant evolution was observed between obtained data of characterized ubnleached and bleached nanofibers.

1. Introduction

The 21st century is the century of paradox, paradox of crisis and transformation. The environmental crisis created by collective unawareness of humanity in conjunction with industrial and technological growth is destroying the planet. The acute condition led researchers all around the world to focus on solutions and create a conscious transforming momentum to open up new grounds and reverse the destruction process. One of the key factors in this reverse process which was previously overlooked is the potential of renewable biomaterials. Trees and plants use air, sunlight and water to process in their "photochemical factories" and generously produce naturally occurring nanocomposites of cellulosic microfibrils embedded in a lignin matrix (Lucia & Rojas, 2009). As a result of recent insight into this nature gift, the great potential of lignocelluloses as nanomaterials came into light. Their unique nanocellulosic structure can be isolated by a top-down approach and tailor-made by a bottom-up approach into multi-functional, and self-assemble into well-defined architectures that are sustainable, renewable, recyclable and environmentally friendly. This issue opens up a great potential for the society industrial and economical sustainable development.

Natural fibers are produced in billions of tons around the world and are therefore abundant, inexpensive and readily available. Kenaf as one of these resources is a feasible source of cellulose which is economically viable and ecologically friendly. Kenaf has a short gestation period of only four months and is a high carbon dioxide absorbent plant (Lam, Hori, & Iiyama, 2003). Kenaf growth does not need pest control while absorbs chemical and heavy metals from the soil. It also has a wider range of adaptation to climates and soils than any other fiber plant in commercial production. Based on comparisons in production, anatomical properties, stem processing, fiber quality, yield and prices, kenaf apparently has multiple advantages compared to hemp, jute, and flax, as a fiber source (Kozlowski, 2000; Rymsza, 2000). In many developing countries such as India, Thailand, and Indonesia the development of kenaf industry may be the key to future advancement of rural areas. In Malaysia the government is heavily promoting the development of kenaf, as the next major industrial crop for the country in line with its policy in developing new sources of economic growth (Khan, 2010).

Kenaf plant contains three types of fiber: bast, core, and pith. The "bast" refers to the outer part of the fiber and represents about 30% of the dry weight of the stalk. Meanwhile, core is the whiter,

* Corresponding author. Tel.: +64 21590016.
E-mail address: samanehkarimi82@gmail.com (S. Karimi).

0144-8617/$ – see front matter © 2013 Elsevier Ltd. All rights reserved.
http://dx.doi.org/10.1016/j.carbpol.2013.09.106

inner part of the fiber, and it contributes around 70% of dry weight of the stalk. The pith consists exclusively of parenchymatous cells, which are not typically prismatic but polygonal in shape (Paridah, Basher, SaifulAzry, & Ahmed, 2011). According to (Faruk, Bledzki, Fink, & Sain, 2012; Liu, Drzal, Mohanty, & Misra, 2007; Zampaloni et al., 2007) the bast fibers have been found to possess attractive mechanical properties that enable their use as alternatives to glass fibers as reinforcing elements in polymer composites.

The hierarchical and multi-level organization of kenaf bast fiber makes the extraction of different types of nanoscale cellulosic fillers possible. Nanofibers extracted from kenaf bast can be incorporated into polymeric matrices and tailor-made to high impact and value-added products. Thus additional research to assess the most effective, industrial viable, and environmentally friendly procedure to extract nanocellulose from these fibers is essential. In this research a top-down chemi-mechanical approach was applied to isolate nanoscale cellulosic fibers from kenaf bast. The data presented in this paper have been meticulously collected to present an accurate quantitative and qualitative comparison between different hierarchy scales of kenaf bast fibers. As a result a comprehensive study and comparison on isolation and characterization of micro to nanoscale cellulosic fibers from kenaf bast has been presented. Researches on nanocellulose isolation from kenaf bast fibers are available (Jonoobi, Harun, Shakeri, Misra, & Oksman, 2009; Kargarzadeh et al., 2012; Shi, Shi, Barnes, & Pittman Jr, 2011; Zaini, Jonoobi, Tahir, & Karimi, 2013). However the applied approach in this research is different. It is worth to note that properties of isolated nanocellulose from the same plant are affected by many factors such as variety, soil, climate, harvest, maturity, retting degree, decortications, disintegration, fiber modification, and technical specification of the isolation process (Kalia et al., 2011). Consequently in order to widespread the application of nanocelluloses extracted from natural fibers, it is necessary to build a reproducible and comprehensive database of their properties and this information is critical before these fibers could reach their highest use potential.

2. Experimental

2.1. Materials

Water retted kenaf (*Hibiscus cannabinus* v36) bast fibers were kindly supplied by the Institute of Tropical Forestry and Forest Products (INTROP, UPM, Malaysia). All used chemicals were purchased from Merck Chemicals (Kuala Lumpur, Malaysia).

2.2. Isolation processes

2.2.1. Chemical treatments

Water retted Kenaf bast fibers coded as RF were cut to short pieces and then cooked in a JSR-212 rotatory digester with 25 wt% NaOH and 0.1 wt% anthraquinone solution (liquor to fiber ratio was 7:1) at 160 °C for 2 h. AQ was added to the cooking liquor to enhance the delignification rate and also protect the fibers from alkali degradation and so called end-wise degradation of cellulosic chains. The obtained pulp was washed and screened thoroughly and divided in two equal parts. In order to remove the residual lignin, one part of the pulped fibers undergone a three-stage bleaching process as described elsewhere (Jonoobi et al., 2009). Bleached and unbleached pulp samples were coded as BP and UBP, respectively.

2.2.2. Mechanical treatment

Extraction of nanofibers from both BP and UBP samples were done by further mechanical destruction using supermasscolloider MKCA 6-3 from Masuko (Japan). Aqueous suspensions of both BP and UBP samples with the concentration of 3 wt% were prepared and blended until formation of a homogeneous mixture. Consequently the suspensions were fed into the grinder and the process repeated until a gel was formed (15 times). The obtained gel from UBP and BP samples were named unbleached nanofiber (UBNF) and bleached nanofiber (BNF), respectively.

2.3. Characterization

2.3.1. Chemical analysis

The chemical composition of RF, UBP and BP samples was analyzed by standard TAPPI methods. Soxhlet extraction (alcohol-acetone) was carried out for 8 h. TAPPI standard 203 om 93 and TAPPI standard 222 om 88 were applied for cellulose and Klason lignin (acid-insoluble) content calculation, respectively. The hemicellulose content was determined according to (Wise, Murphy, & d'Addieco, 1946).

2.3.2. Morphological analysis

The morphology of RF, BP and UBP samples was investigated using a JEOL JSM-6400 scanning electron microscope (SEM). All samples were sputter coated with gold to avoid charging.

The structure and size of the obtained nanofibers was studied by transmission electron microscopy (TEM) on a Hitachi model H-7100. A drop of the diluted UBNF and BNF suspensions was deposited on a carbon-coated grid. To enhance the contrast, samples were stained using 2% (*w*/*w*) uranyl acetate solution and allowed to dry at room temperature.

Measurements of fibers dimensions on obtained micrographs were done using the attached image analyzer software. At least 50 measurements from each sample were done. The results were reported as the mean values of the data for each set of measurements.

2.3.3. Functional group analysis

Fourier transform infrared (FTIR) spectroscopy studies were performed on a Perkin-Elmer spectrometer 100 series in order to determine changes in functional groups that may have been caused by the treatments. The universal attenuated total reflectance (UATR) sampling accessories were used. Transmittance mode was within the range of 4000–280 cm^{-1}.

2.3.4. Crystallinity determination

X-ray diffraction measurements were conducted using X'pert Pro Panalytical PW 3040 MPD diffractometer. 2θ range was between 4° and 60°. Phase recognition of the samples was achieved by use of the X'pert Highscore software with support of the ICDD-PDF-2 database.

Crystallinity of all samples was determined and the crystallinity index (CrI) was calculated by an empirical method using the Eq. (1) (Segal et al., 1959):

$$\mathrm{CrI\%} = \left(\frac{I_{002} - I_{am}}{I_{002}}\right) \times 100 \quad (1)$$

where I_{002} is the maximum intensity of the (0 0 2) lattice diffraction peak and I_{am} is the intensity scattered by the amorphous part of the sample.

2.3.5. Thermogravimetric analysis (TGA)

Thermogravimetric analysis was carried out using a TGA Q500 instrument to determine the thermal stability and decomposition temperature of samples. Data were obtained under linear temperature conditions. The temperature was swept from room temperature to 500 °C at a heating rate of 10 °C/min under nitrogen atmosphere.

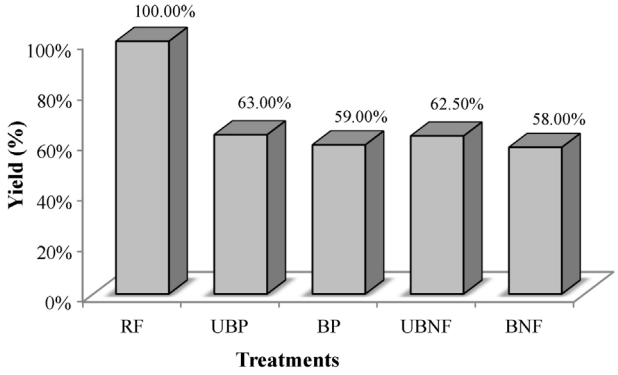

Fig. 1. Yields of obtained materials after each treatment.

3. Results and discussion

3.1. Yields

Yields of the resulting material at each stage were calculated by weighing the oven-dried material (UBP and BP) or freeze-dried (UBNF and BNF) against the oven-dried weight of the starting material (RF). Achieved data are presented in Fig. 1.

It is worth to note that the nanocellulose yield in the present work was significantly higher than two similar works (Kargarzadeh et al., 2012; Shi et al., 2011) which used the same starting material (kenaf bast) for nanocellulose isolation, but applied an all chemical approach.

Presented data are validating the effectiveness of applied approach in this research and highlights the efficiency of the mechanical process. It is worth to note that producing nanocellulose by mechanical force, apart from its impeccable yield have other benefits such as; ease of the process (producing nanofiber in a single step), energy efficiency (Jonoobi, Mathew, & Oksman, 2012), viable for industrial capacity production, less chemical usage, environmental concerns and wastewater issue in regard to industrial production.

3.2. Chemical composition

The chemical composition of the kenaf fibers after cooking and bleaching procedures is presented in Table 1.

The purpose of the pulping and consecutive bleaching processes was to dissolve and eliminate lignin and hemicellulose from the matrix surrounding the cellulose microfibrils, and isolate individual microfibers. As a result it is obvious that raw kenaf bast fibers should have the highest percentage of hemicellulose and lignin and the lowest percentage of cellulose. The pulping procedure was found to efficiently remove lignin and hemicellulose from kenaf bast fibers, as indicated by a reduction in lignin content from 12.9 to 2.6 wt% and hemicellulose content from 18.5 to 11.2 wt%. The bleaching treatment decreased the residual lignin and hemicellulose content as shown in Table 1. As expected, the final fibers obtained after the bleaching process were found to have the highest cellulose content of 91.8 wt%. Obtained data are in range of reported data in the literature (Jonoobi et al., 2009; Kargarzadeh et al., 2012; Rowell, Han, & Rowell, 2000; Shi et al., 2011; Swingle, Urias, Doyle, & Voigt, 1978).

Table 1
Chemical composition of the kenaf fibers after different treatments.

Component (%)	RF	UBP	BP
Cellulose	61.2 ± 0.8	82.3 ± 0.6	91.8 ± 0.9
Hemicelluloses	18.5 ± 1.5	11.2 ± 1.5	4.9 ± 0.4
Lignin	12.9 ± 0.7	2.6 ± 0.2	0.5 ± 0.1

3.3. Morphological analysis

Fig. 2A–H illustrates how the fiber morphology was changed from the micro to nanoscale by the applied procedures. They clearly present the hierarchical structure of kenaf bast fibers and the way each step of treatment disintegrates fibrillar bundles. Fig. 2.B demonstrates a single fiber from Fig. 2A under SEM and shows how a single raw fiber is composed of individual microfibers linked together by lignin and hemicellulose. SEM micrograph of obtained fiber after pulping process is shown in Fig. 2C. The diameter of isolated fibers at this stage ranged from 2.09 to 22.9 μm. These fibers were further individualized by chemical treatment in the bleaching process (Fig. 2D). At this stage the diameter range of disintegrated fibers was from 1.94 to 21.1 μm. At this point, in order to extract nanoscale cellulosic fiber, intensive mechanical treatment by Masuko grinder was applied. Color and texture of the formed UBNF and BNF gels are shown in Fig. 2E and F while the morphology of the resultant nanofibers under TEM is illustrated in Fig. 2G and H, respectively. The diameter range of isolated UBNF was from 2.2 to 34 nm while the diameter of BNF samples ranged from 1.2 to 30.02 nm. Obtained data demonstrate that the selected pulping process was very effective in liberating fibers as well as dissolving lignin and hemicellulose. This process reduced the average diameter of fibers by almost 80%. The result of chemical composition (Table 1) also confirms this assertion. During the bleaching process the remained lignin and hemicellulose washed out and caused further defibrillation of cooked fibers. However, the average diameter reduction was only 7.14%. Considering the principals of green chemistry, consumed time and energy as well as produced wastewater during this process, it may not be worthy especially when applied to industrial scales. This implies more consideration in deciding on the necessity of bleaching process. Applied mechanical treatment effectively and efficiently disintegrates fibrillar bundles rendering nanoscale cellulosic fibers even without prebleaching treatment. Comparing obtained data with available literature on nanocellulose morphology isolated from kenaf bast demonstrates the effectiveness of the applied approach to defibrillate the fibers on a nanoscale level. Table 2 abbreviated this information.

3.4. Fourier transform infrared (FTIR) spectroscopy

FTIR spectroscopy involves the interaction of energy and matter. By recording the magnitude of absorbed energy and comparing it with available database, the present functional groups can be identified and chemical structure of the sample can be characterized. This characterization was carried out for all samples to understand the effect of each treatment on the chemical structure of obtained material. Fig. 3A depicted the achieved IR spectra while specific absorption peaks for each particular component have been identified in Table 3.

The absorbance peaks in the 3300–3400 cm^{-1} region corresponds to free O—H stretching and bending vibration of the OH groups of cellulose (Blackwell, Vasko, & Koenig, 1970; Edwards, Farwell, & Williams, 1994; Edwards, Farwell, & Webster, 1997; Nelson & O'Connor, 1964). The peaks around 2900–2800 cm^{-1} are due to the stretching of C—H (Le Troedec et al., 2008; Sain & Panthapulakkal, 2006). The peak located at 1731 cm^{-1} in the RF spectra is attributed to the C=O stretching vibration of the acetyl group in hemicellulose, pectin or the ester linkage of carboxylic group in the ferulic and p-coumeric acids of lignin and/or hemicellulose (Ahmad, Mosadeghzad, Daik, & Ramli, 2008; Alemdar & Sain, 2008; Sain & Panthapulakkal, 2006; Sun, Xu, Sun, Fowler, & Baird, 2005; Zuluaga et al., 2009). This peak disappeared completely in the UBP, BP, UBNF and BNF spectra indicating the removal of lignin and most of the hemicellulose during the chemical treatments and

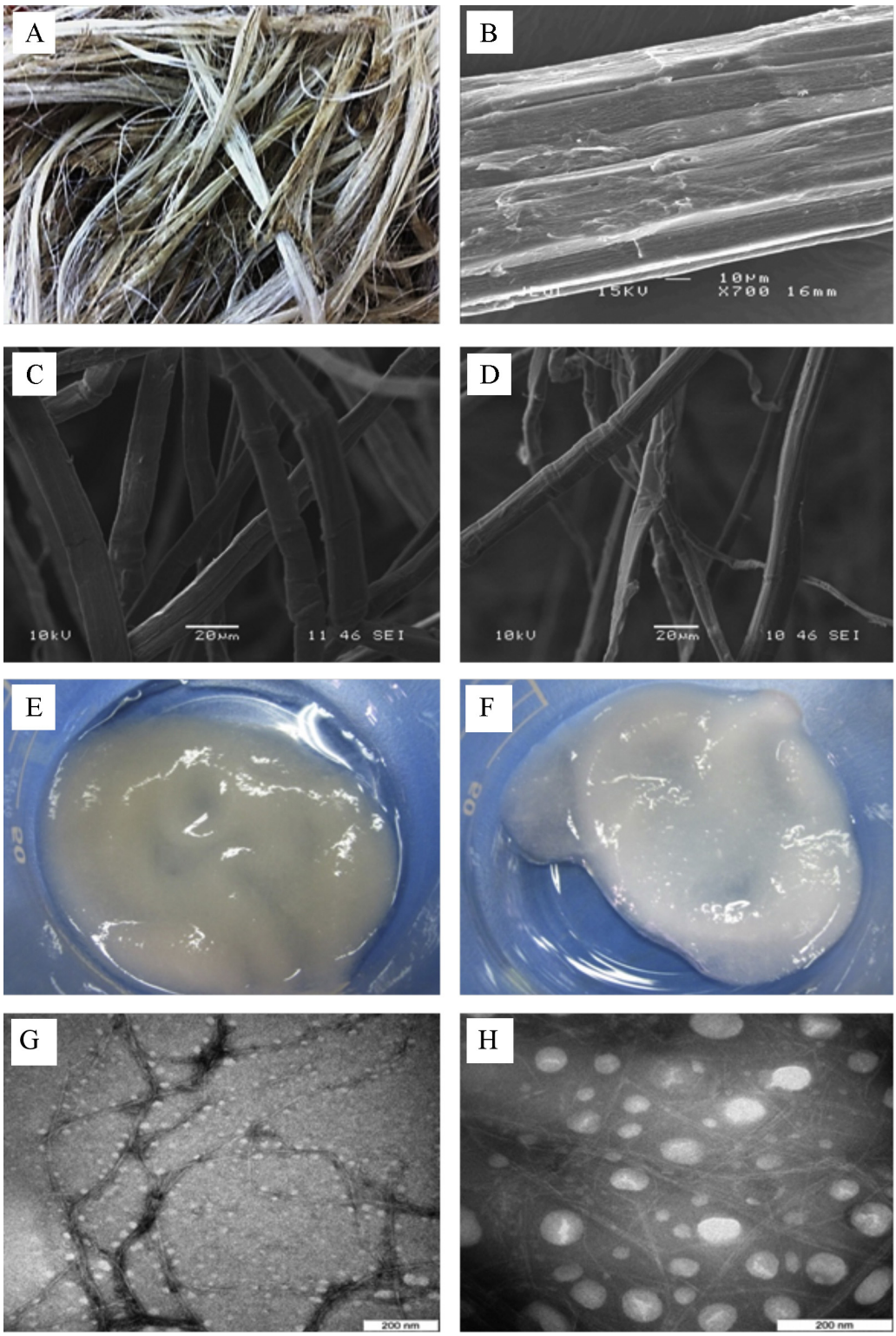

Fig. 2. (A) Photograph of primary RF, (B) SEM micrograph of RF, (C) SEM micrograph of UBP, (D) SEM micrograph of BP, (E) obtained gel from UBNF, (F) obtained gel from BNF, (G) TEM micrograph of UBNF and (H) TEM micrograph of BNF.

during severe mechanical treatment of nanofiber preparation. The peaks observed at 1630 and 1640 cm^{-1} in the spectra of all samples are attributed to the O—H bending of adsorbed water (Jiang & Hsieh, 2013; Le Troedec et al., 2008; Nacos et al., 2006). The absorbance in the 1425–1435 cm^{-1} regions of RF, UBP and BP samples is associated to the CH_2 symmetric bending and/or C=C stretching in aromatic groups of pectin, lignin, and/or hemicellulose (Le Troedec et al., 2008). The 1242 cm^{-1} peak in the spectra of RF sample was associated to the C—O stretching of the aryl group in lignin (Jonoobi et al., 2009; Kargarzadeh et al., 2012) and disappearance of this peak in the UBP, BP, UBNF and BNF is regarded to the removal of lignin after the pulping process.

The differences between the FTIR spectrums in the hierarchy of kenaf bast fiber clearly indicate the effectiveness of applied

Table 2
Obtained morphological data in contrast with other studies.

Treatment	Method	Diameter range	Average diameter	Reference
RF	–	15.5–148 μm	55.18 μm	This study
		49.9–115.5 μm	82.7 μm	Kargarzadeh et al. (2012)
		10–80 μm	–	Jonoobi et al. (2009)
UBP	Alkali treatment	2.09–22.9 μm	11.37 μm	This study
		20–90 μm	–	Zaini et al. (2013)
		20.7–60.7 μm	40.7 μm	Kargarzadeh et al. (2012)
BP	Bleaching process	1.94–21.1 μm	10.56 μm	This study
		8–14 μm	11 μm	Zaini et al. (2013)
		7.4–11 μm	9.2 μm	Kargarzadeh et al. (2012)
		8.58–12.68 μm	10.63 μm	Shi et al. (2011)
UBNF	Grinding	2.2–34 nm	7.05 nm	This study
	Homogenization	10–90 nm	–	Jonoobi et al. (2009)
BNF	Grinding	1.2–30.02 nm	6.03 nm	This study
	Acid hydrolysis	2–5 nm	–	Zaini et al. (2013)
	Homogenization	10–70 nm	–	Jonoobi et al. (2009)
	Acid hydrolysis	8.6–15.4 nm	12 nm	Kargarzadeh et al. (2012)
	Acid hydrolysis	13.32–56.18 nm	34.75 nm	Shi et al. (2011)

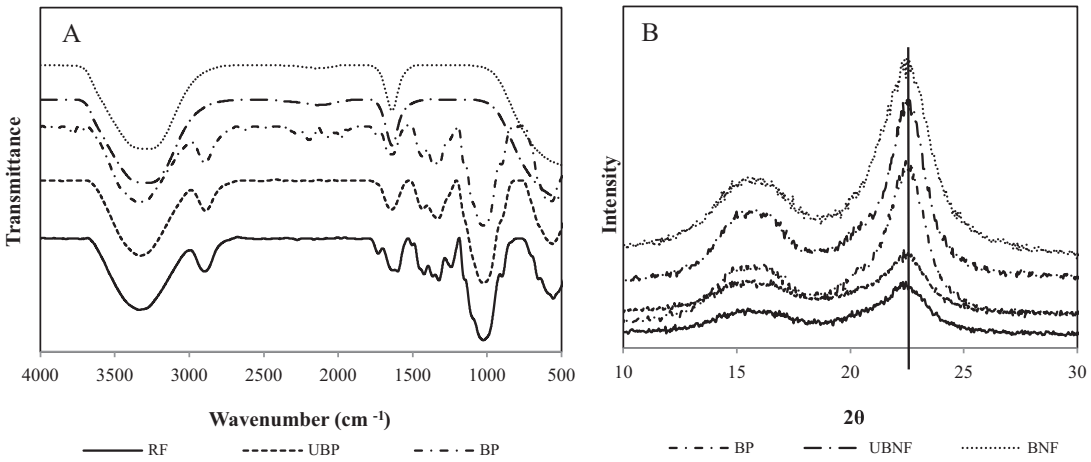

Fig. 3. (A) FTIR spectra of samples and (B) X-ray diffraction patterns of samples.

procedures and it is evident that there was no remaining lignin in the obtained UBNF and BNF samples. This confirms successful extraction of UBNF and BNF nanofibers and highlights the similarity of their spectrum.

3.5. Crystallinity

In order to determine the crystallinity of the fibers and effect of each treatment on the resulting material, X-ray diffractometry (XRD) was carried out. Fig. 3B presents the obtained XRD patterns for kenaf bast fibers at different stages of purification. The fiber crystallinity index at each stage was calculated and presented in Table 4.

As shown in Fig. 3B all samples presented behavior typical of semi-crystalline materials. An amorphous broad hump at 2θ value of 16° and crystalline peaks at 2θ value of 22.5° was observed. It could be noticed that cellulose was present in the form of cellulose I, and not cellulose II. Cellulose I X-ray diffraction pattern is characterized by main signal at 2θ value of 22.5° attributed to diffraction plane 0 0 2 (Bhatnagar & Sain, 2005; Dufresne, 2012; Klemm, Heublein, Fink, & Bohn, 2005; Morán, Alvarez, Cyras, & Vázquez, 2008). As expected, the magnitudes of the crystalline peak and crystallinity index goes on increasing from the raw kenaf bast fibers to nanofiber due to purification of cellulose and removal of amorphous lignin and hemicellulose.

Table 3
FTIR main transitions for isolated fibers and the assignment of the IR bands of functional groups.

Wave number (cm^{-1})	Appearance	Functional group	Component
3400–3300	All samples	OH	Cellulose
2900	RF, UBP, BP	C—H	Lignin
1726	RF	C=O	Hemicellulose, lignin
1640	All samples	OH	Adsorbed water
1435–1425	RF, UBP, BP	CH_2, C=C	Pectin, lignin, hemicellulose
1325–1315	RF, UBP, BP	C—H, O—H	Hemicellulose, OH phenolic in lignin
1244	RF	C—O	Lignin
1055–1025	RF, UBP, BP	Aromatic	Lignin
897–895	RF, UBP, BP	C—H	Polysaccharides, lignin

Table 4
Determined degradation temperature (T_{max}) and crystallinity index (CI) after each stage of purification in contrast with other works.

Sample	T_{max} (°C)	CI (%)	Reference
RF	325	62.9	This study
	321	67	Zaini et al. (2013)
	328	60.8	Kargarzadeh et al. (2012)
	313	48.2	Jonoobi et al. (2009)
	–	63.8	Shi et al. (2011)
UBP	335.8	72.1	This study
	368	77	Zaini et al. (2013)
	350	68.2	Kargarzadeh et al. (2012)
	321	68.1	Jonoobi et al. (2009)
	–	–	Shi et al. (2011)
BP	338.9	77.2	This study
	346	79	Zaini et al. (2013)
	350	72.8	Kargarzadeh et al. (2012)
	342	77.3	Jonoobi et al. (2009)
	–	68.9	Shi et al. (2011)
UBNF	357.9	79.4	This study
	348	79.2	Jonoobi et al. (2009)
BNF	361	81.5	This study
	317[a]	84	Zaini et al. (2013)
	358[b]		
	218[c]	81.8	Kargarzadeh et al. (2012)
	358[d]		
	351	81.4	Jonoobi et al. (2009)
	–	83.9	Shi et al. (2011)

[a] Sulfuric acid hydrolyzed nanocellulose.
[b] HCl hydrolyzed nanocellulose.
[c] Sulfated cellulose from sulfuric acid hydrolyzed nanocellulose.
[d] Unsulfated cellulose from sulfuric acid hydrolyzed nanocellulose.

A crystallinity index of 62.9% was reported for the raw kenaf bast fibers which is typical of fibers from a secondary wall. Obtained results confirm that the non-cellulosic amorphous polysaccharides were efficiently removed by the applied alkali and consecutive bleaching processes. Pulping process eliminated lignin and hemicelluloses, so that the percentage of the crystalline regions in the material increased. Also, while bleaching process accelerated the cleavage of the cellulose molecular chains within the amorphous regions it consequently increased the crystallinity of the bleached fibers. The results also demonstrated the effectiveness of the applied mechanical treatment as it led to dissolve the remaining impurities and improved crystallinity for both bleached and unbleached nanofibers significantly. As presented in Table 4 achieved data well agreed with the literature.

3.6. TGA analysis

Thermogravimetric analysis (TGA) was carried out for all samples in order to investigate the effect of each treatment on material decomposition and thermal stability through samples mass change. This is a critical issue in suitability of the kenaf fibers for biocomposite processing. Processing of many types of thermoplastic polymers require temperatures greater than 200 °C. According to Fisher, Hajaligol, Waymack, and Kellogg (2002) the primary thermal decomposition of cellulosic materials occurs between 200 and 400 °C.

Acquired TGA and derivative TG curves of samples are presented in Fig. 4A and B, respectively. Moreover abbreviated results as well as comparison with similar works are collected in Table 4. One-stage decomposition curve which is typical in TG curves can be seen in Fig. 4A and stability limit of samples can be defined easily. The derivative TG (DTG) curve is a plot of d_m/d_t versus temperature and its peak clearly identifies the temperature at which mass loss is at a maximum. An initial weight loss of approximately 5% was observed for all samples upon heating to 100 °C. It is attributed to

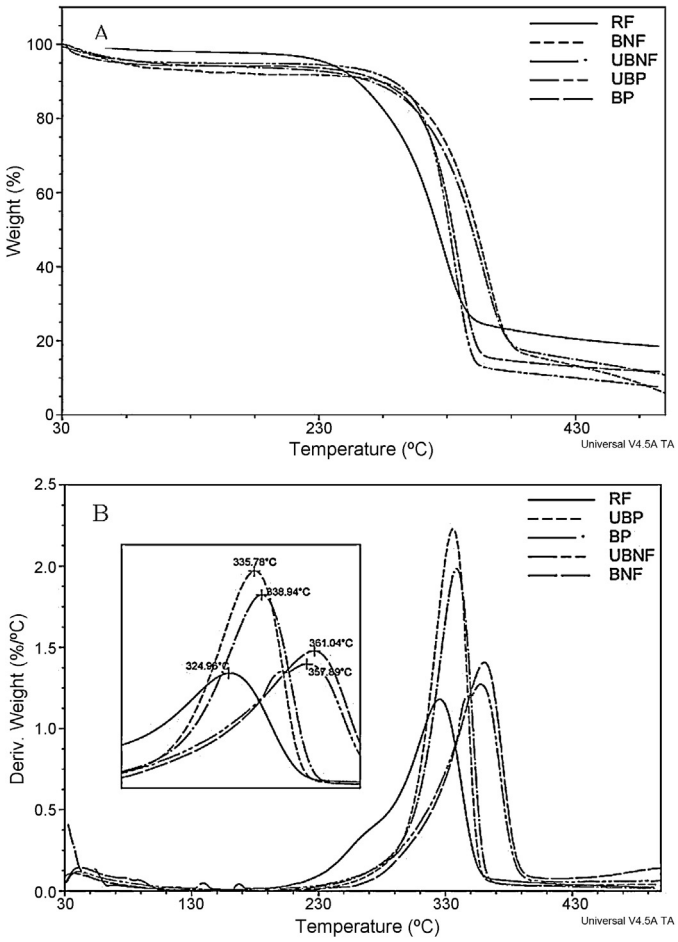

Fig. 4. (A) TG and (B) DTG curves of samples.

evaporation of loosely bound moisture on the surfaces of samples. Higher amount of residue in the raw kenaf fiber as opposed to the treated fibers is observed. It is due to the presence of ash as well as lignin, which have low degradation rate (Ashori, Harun, Raverty, & Yusoff, 2006; Jonoobi et al., 2009; Yang, Yan, Chen, Lee, & Zheng, 2007).

A low temperature a shoulder can be observed in the DTG curve of RF which is attributed to the presence of hemicellulose (Rosa et al., 2010) and its removal in the curves for other samples is due to hemicellulose removal during the applied treatments. These results are in agreement with the chemical composition and FTIR analyses. Based on the results, the thermal stability of kenaf fibers is increased by the applied chemi-mechanical treatments. Removal of non-cellulosic constituent of raw fiber in each treatment helps to make the cellulose structure more dense and compact and cause the rise in the degradation temperature of samples accordingly. Thermal stability of extracted UBNF and BNF samples is increased by 9.82% and 10.79%, respectively, compared to RF sample. The maximum temperature peak for RF sample is attributed to the thermal degradation of hemicellulose, while the corresponding peak for the other samples indicated the decomposition of cellulose (Morán et al., 2008; Yang et al., 2007). It is well known that hemicellulose decomposes before lignin and cellulose. Low thermal stability of hemicellulose could be attributed to the presence of acetyl groups (Shebani, Van Reenen, & Meincken, 2008). No significant evolution was reported for the degradation temperature of UBNF and BNF samples. Thermal stability of BNF samples only increased by 0.88% compared with UBNF samples.

It is worth to note that generally lower thermal stabilities compared to raw sample have been reported in previous studies (Aggarwal & Dollimore, 1997; Fahma, Iwamoto, Hori, Iwata, & Takemura, 2010; Jain, Lal, & Bhatnagar, 1986; Kargarzadeh et al., 2012; Kim & Kuga, 2001; Roman & Winter, 2004; Varma & Chavan, 1995; Vicini et al., 2004; Wang, Ding, & Cheng, 2007) which used chemical methods to extract cellulose and nanocellulose. Stated causes for the lowering in cellulose degradation temperature include molecular weight degradation of chemically treated cellulose as well as the increase in the amount of short cellulose chains resulting in lowered thermal degradation energies (Johnson, 2010; Kargarzadeh et al., 2012; Wang et al., 2007). Moreover, increased surface reactivity of cellulose by the attached, highly reactive functional groups can be an explanation (Saïd Azizi Samir, Alloin, Paillet, & Dufresne, 2004). However, this lowering in thermal stability is not an issue when nanocellulose is isolated by mechanical shearing. Obtained results as well as studies done by Jonoobi et al. (2009, 2010, 2011a) and Jonoobi, Khazaeian, Tahir, Azry, and Oksman (2011) is confirming this statement.

4. Conclusions

Kenaf bast cellulosic fibers were isolated hierarchically in three distinct stages. First, the raw fibers were subjected to a conventional alkali pulping process, obtained pulped fibers then undergone a bleaching process and finally both pulped and bleached fibers were mechanically separated into their constituent nanoscale cellulosic fibers. Microscopy studies revealed that applied procedures successfully isolated nanoscale cellulosic fibers from both unbleached and bleached pulps. Unbleached and bleached nanofibers yielded 62.5% and 58%, respectively. The analysis of the chemical composition indicated an increase in the cellulose content after each treatment. FTIR spectra also confirmed this data and revealed that the chemical treatments successfully removed lignin and hemicellulose. Both XRD and TGA results indicated progressive enhancement of properties in fibers, hierarchically, in going from RF to BNF. This was believed to be due to the removal of hemicellulose and lignin as well as the boost in crystallinity of the samples during applied procedures. Finally obtained results as well as comparison with other works demonstrated the effectiveness and superiority of the applied approach. The interesting highlight of this research was achieved data on unbleached nanofiber which offers the probable redundancy of the bleaching process. Elimination of the bleaching procedures in the nanocellulose isolation process is of great benefit and importance as the effluent from the bleaching process contains oxidized lignin, carbohydrates, and a range of organochlorine compounds. Some organochlorines break down quickly and some including dioxins and furans have long lives and are seriously detrimental to the environment as well as human health. However the surface chemistry of achieved unbleached and bleached nanofibers is different and it may lead to different behavior when incorporated into polymeric matrices. A future goal is to use these two types of nanofibers as reinforcing elements with a biodegradable thermoplastic. Then their performance will be studied and compared in a subsequent report.

Acknowledgements

Authors would like to thank Dr. Mehdi Jonoobi for his sincere help in obtaining nanofiber samples. Many thanks are also expressed to Mr. Mehdi Hassani for his faithful support and assistance in editing the manuscript. Thanks to the Institute of Tropical Forestry and Forest Products (INTROP) for financial and technical support of the research.

Appendix A. Supplementary data

Supplementary data associated with this article can be found, in the online version, at http://dx.doi.org/10.1016/j.carbpol.2013.09.106.

References

Aggarwal, P., & Dollimore, D. (1997). The combustion of starch, cellulose and cationically modified products of these compounds investigated using thermal analysis. *Thermochimica Acta*, *291*(1), 65–72.
Ahmad, I., Mosadeghzad, Z., Daik, R., & Ramli, A. (2008). The effect of alkali treatment and filler size on the properties of sawdust/UPR composites based on recycled PET wastes. *Journal of Applied Polymer Science*, *109*(6), 3651–3658.
Alemdar, A., & Sain, M. (2008). Isolation and characterization of nanofibers from agricultural residues: Wheat straw and soy hulls. *Bioresource Technology*, *99*(6), 1664–1671.
Ashori, A., Harun, J., Raverty, W. D., & Yusoff, M. N. M. (2006). Chemical and morphological characteristics of Malaysian cultivated kenaf (*Hibiscus cannabinus*) fiber. *Polymer-Plastics Technology and Engineering*, *45*(1), 131–134.
Bhatnagar, A., & Sain, M. (2005). Processing of cellulose nanofiber-reinforced composites. *Journal of Reinforced Plastics and Composites*, *24*(12), 1259–1268.
Blackwell, J., Vasko, P. D., & Koenig, J. L. (1970). Infrared and Raman spectra of the cellulose from the cell wall of *Valonia ventricosa*. *Journal of Applied Physics*, *41*(11), 4375–4379.
Dufresne, A. (2012). *Nanocellulose: From nature to high performance tailored materials*. Berlin, Germany: Walter de Gruyter.
Edwards, H. G. M., Farwell, D. W., & Williams, A. C. (1994). FT-Raman spectrum of cotton: A polymeric biomolecular analysis. *Spectrochimica Acta Part A: Molecular Spectroscopy*, *50*(4), 807–811.
Edwards, H. G. M., Farwell, D. W., & Webster, D. (1997). FT-Raman microscopy of untreated natural plant fibres. *Spectrochimica Acta Part A: Molecular and Biomolecular Spectroscopy*, *53*(13), 2383–2392.
Fahma, F., Iwamoto, S., Hori, N., Iwata, T., & Takemura, A. (2010). Isolation, preparation, and characterization of nanofibers from oil palm empty-fruit-bunch (OPEFB). *Cellulose*, *17*(5), 977–985.
Faruk, O., Bledzki, A. K., Fink, H. P., & Sain, M. (2012). Biocomposites reinforced with natural fibers: 2000–2010. *Progress in Polymer Science*, *37*(11), 1552–1596.
Fisher, T., Hajaligol, M., Waymack, B., & Kellogg, D. (2002). Pyrolysis behavior and kinetics of biomass derived materials. *Journal of Analytical and Applied Pyrolysis*, *62*(2), 331–349.
Jain, R. K., Lal, K., & Bhatnagar, H. L. (1986). Thermal studies on C-6 substituted cellulose and its subsequent C-2 and C-3 esterified products in air. *European Polymer Journal*, *22*(12), 993–1000.
Jiang, F., & Hsieh, Y. L. (2013). Chemically and mechanically isolated nanocellulose and their self-assembled structures. *Carbohydrate Polymers*, *95*(1), 32–40.
Johnson, R. K. (2010). *TEMPO-oxidized nanocelluloses: Surface modification and use as additives in cellulosic nanocomposites*. Virginia Polytechnic (Doctoral Dissertation)
Jonoobi, M., Harun, J., Shakeri, A., Misra, M., & Oksman, K. (2009). Chemical composition, crystallinity, and thermal degradation of bleached and unbleached kenaf bast (*Hibiscus cannabinus*) pulp and nanofibers. *BioResources*, *4*(2), 626–639.
Jonoobi, M., Harun, J., Tahir, P. M., Zaini, L. H., SaifulAzry, S., & Makinejad, M. D. (2010). Characteristic of nanofiber extracted from kenaf core. *BioResources*, *5*(4), 2556–2566.
Jonoobi, M., Harun, J., Tahir, P. M., Shakeri, A., SaifulAzry, S., & Makinejad, M. D. (2011). Physicochemical characterization of pulp and nanofibers from kenaf stem. *Materials Letters*, *65*(7), 1098–1100.
Jonoobi, M., Khazaeian, A., Tahir, P. M., Azry, S. S., & Oksman, K. (2011). Characteristics of cellulose nanofibers isolated from rubberwood and empty fruit bunches of oil palm using chemo-mechanical process. *Cellulose*, *18*(4), 1085–1095.
Jonoobi, M., Mathew, A. P., & Oksman, K. (2012). Producing low-cost cellulose nanofiber from sludge as new source of raw materials. *Industrial Crops and Products*, *40*(1), 232–238.
Kalia, S., Dufresne, A., Cherian, B. M., Kaith, B. S., Avérous, L., Njuguna, J., & Nassiopoulos, E. (2011). Cellulose-based bio-and nanocomposites: A review. *International Journal of Polymer Science*, *2011*, 1–35.
Kargarzadeh, H., Ahmad, I., Abdullah, I., Dufresne, A., Zainudin, S. Y., & Sheltami, R. M. (2012). Effects of hydrolysis conditions on the morphology, crystallinity, and thermal stability of cellulose nanocrystals extracted from kenaf bast fibers. *Cellulose*, *19*(3), 855–866.
Khan, A. R. (2010). Kenaf, a fiber for future: The Harusmas experience. *JEC Composite Magazine*, 21–23.
Kim, U. J., & Kuga, S. (2001). Thermal decomposition of dialdehyde cellulose and its nitrogen-containing derivatives. *Thermochimica Acta*, *369*(1), 79–85.
Klemm, D., Heublein, B., Fink, H. P., & Bohn, A. (2005). Cellulose: Fascinating biopolymer and sustainable raw material. *Angewandte Chemie International Edition*, *44*(22), 3358–3393.
Kozlowski, R. (2000). Potential and diversified uses of green fibres. In *Paper presented at the third international wood and natural fibres composites symposium* Kassel, Germany, (19th–20th September).
Lam, T. B. T., Hori, K., & Iiyama, K. (2003). Structural characteristics of cell walls of kenaf (*Hibiscus cannabinus* L.) and fixation of carbon dioxide. *Journal of Wood Science*, *49*(3), 255–261.

Le Troedec, M., Sedan, D., Peyratout, C., Bonnet, J. P., Smith, A., Guinebretiere, R., loaguen, V., & Krausz, P. (2008). Influence of various chemical treatments on the composition and structure of hemp fibres. *Composites Part A: Applied Science and Manufacturing*, *39*(3), 514–522.

Liu, W., Drzal, L. T., Mohanty, A. K., & Misra, M. (2007). Influence of processing methods and fiber length on physical properties of kenaf fiber reinforced soy based biocomposites. *Composites Part B: Engineering*, *38*(3), 352–359.

Lucia, L. A., & Rojas, O. J. (2009). *The nanoscience and technology of renewable biomaterials*. Wiley Online Library.

Morán, J. I., Alvarez, V. A., Cyras, V. P., & Vázquez, A. (2008). Extraction of cellulose and preparation of nanocellulose from sisal fibers. *Cellulose*, *15*(1), 149–159.

Nacos, M., Katapodis, P., Pappas, C., Daferera, D., Tarantilis, P., Christakopoulos, P., & Polissiou, M. (2006). Kenaf xylan – A source of biologically active acidic oligosaccharides. *Carbohydrate Polymers*, *66*(1), 126–134.

Nelson, M. L., & O'Connor, R. T. (1964). Relation of certain infrared bands to cellulose crystallinity and crystal latticed type. Part I: Spectra of lattice types I, II, III and of amorphous cellulose. *Journal of Applied Polymer Science*, *8*(3), 1311–1324.

Paridah, M. T., Basher, A. B., SaifulAzry, S., & Ahmed, Z. (2011). Retting process of some bast plant fibers and its effect on fiber quality: A review. *BioResources*, *6*(4), 5260–5281.

Roman, M., & Winter, W. T. (2004). Effect of sulfate groups from sulfuric acid hydrolysis on the thermal degradation behavior of bacterial cellulose. *Biomacromolecules*, *5*(5), 1671–1677.

Rosa, M. F., Medeiros, E. S., Malmonge, J. A., Gregorski, K. S., Wood, D. F., Mattoso, L. H. C., Glenn, G., Orts, W. J., & Imam, S. H. (2010). Cellulose nanowhiskers from coconut husk fibers: Effect of preparation conditions on their thermal and morphological behavior. *Carbohydrate Polymers*, *81*(1), 83–92.

Rowell, R. M., Han, J. S., & Rowell, J. S. (2000). Characterization and factors effecting fiber properties. In A. L. L. Elisabete Frollini, H. C. Luiz, & Mattoso (Eds.), *Natural polymers and agrofibers bases composites* (pp. 115–134). Sao Carlos, Brazil: Embrapa Agricultural Instrumentation.

Rymsza, T. A. (2000). *Advancements of kenaf in the USA kenaf paper and nonpaper developments*.

Saïd Azizi Samir, M. A., Alloin, F., Paillet, M., & Dufresne, A. (2004). Tangling effect in fibrillated cellulose reinforced nanocomposites. *Macromolecules*, *37*(11), 4313–4316.

Sain, M., & Panthapulakkal, S. (2006). Bioprocess preparation of wheat straw fibers and their characterization. *Industrial Crops and Products*, *23*(1), 1–8.

Segal, L. G. J. M. A., Creely, J. J., Martin, A. E., & Conrad, C. M. (1959). An empirical method for estimating the degree of crystallinity of native cellulose using the X-ray diffractometer. *Textile Research Journal*, *29*(10), 786–794.

Shebani, A. N., Van Reenen, A. J., & Meincken, M. (2008). The effect of wood extractives on the thermal stability of different wood species. *Thermochimica Acta*, *471*(1), 43–50.

Shi, J., Shi, S. Q., Barnes, H. M., & Pittman, C. U., Jr. (2011). A chemical process for preparing cellulose fibers hierarchically from kenaf bast fibers. *BioResources*, *6*(1), 879–890.

Sun, X. F., Xu, F., Sun, R. C., Fowler, P., & Baird, M. S. (2005). Characteristics of degraded cellulose obtained from steam-exploded wheat straw. *Carbohydrate Research*, *340*(1), 97–106.

Swingle, R. S., Urias, A. R., Doyle, J. C., & Voigt, R. L. (1978). Chemical composition of kenaf forage and its digestibility by lambs and in vitro. *Journal of Animal Science*, *46*(5), 1346–1350.

Varma, A. J., & Chavan, V. B. (1995). Thermal properties of oxidized cellulose. *Cellulose*, *2*(1), 41–49.

Vicini, S., Princi, E., Luciano, G., Franceschi, E., Pedemonte, E., Oldak, D., Kaczmarek, H., & Sionkowska, A. (2004). Thermal analysis and characterisation of cellulose oxidised with sodium methaperiodate. *Thermochimica Acta*, *418*(1), 123–130.

Wang, N., Ding, E., & Cheng, R. (2007). Thermal degradation behaviors of spherical cellulose nanocrystals with sulfate groups. *Polymer*, *48*(12), 3486–3493.

Wise, L. E., Murphy, M., & d'Addieco, A. A. (1946). Chlorite holocellulose, its fractionation and bearing on summative wood analysis and on studies on the hemicelluloses. *Paper Trade Journal*, *122*(2), 35.

Yang, H., Yan, R., Chen, H., Lee, D. H., & Zheng, C. (2007). Characteristics of hemicellulose, cellulose and lignin pyrolysis. *Fuel*, *86*(12), 1781–1788.

Zaini, L. H., Jonoobi, M., Tahir, P. M., & Karimi, S. (2013). Isolation and characterization of cellulose whiskers from kenaf (*Hibiscus cannabinus* L.) bast fibers. *Journal of Biomaterials and Nanobiotechnology*, *4*, 37–44.

Zampaloni, M., Pourboghrat, F., Yankovich, S. A., Rodgers, B. N., Moore, J., Drzal, L. T., Mohanty, A. K., & Misra, M. (2007). Kenaf natural fiber reinforced polypropylene composites: A discussion on manufacturing problems and solutions. *Composites Part A: Applied Science and Manufacturing*, *38*(6), 1569–1580.

Zuluaga, R., Putaux, J. L., Cruz, J., Vélez, J., Mondragon, I., & Gaṇán, P. (2009). Cellulose microfibrils from banana rachis: Effect of alkaline treatments on structural and morphological features. *Carbohydrate Polymers*, *76*(1), 51–59.